



---

# OPTIMIZATION OF POWER CONTROL TO ENSURE STABLE ELECTRICITY SUPPLY IN MICRO-HYDRO POWER PLANT

By

Nota Effiandi<sup>1</sup>, Rahmat Hafiz<sup>2</sup>, Mutiara Efendi<sup>3</sup>, Vamellia Sari Indah Negara<sup>4</sup>, Reodhy Hamzah<sup>5</sup>

<sup>1,2,3,4,5</sup>Department of Mechanical Engineering, Polytechnic State of Padang, Indonesia

Email: <sup>2</sup>[rahmathafiz@pnp.ac.id](mailto:rahmathafiz@pnp.ac.id)

---

## Article Info

### Article history:

Received Oct 18, 2025

Revised Oct 22, 2025

Accepted Nov 11, 2025

---

### Keywords:

Micro-hydro; Power Control;  
Voltage Stability; Frequency  
Regulation; Optimization

---

## ABSTRACT

A This study proposes an optimization-based power control strategy to enhance voltage and frequency stability in micro-hydro power plants (MHPP). The approach integrates multi-objective optimization, adaptive control, predictive algorithms, and robust mechanisms to overcome instability caused by load and water flow variations. System modeling and simulation were performed in MATLAB/Simulink, followed by experimental validation on a laboratory-scale prototype. Results show significant improvements compared to conventional PID and fixed-gain Electronic Load Controllers (ELC), reducing voltage and frequency deviations by up to 69% and 67%, respectively. Total Harmonic Distortion (THD) decreased to 3.8%, power factor improved to 0.93, and overall efficiency reached 87.2%. The method proved effective, stable, and feasible for real-time microcontroller implementation, offering a reliable solution for isolated and rural MHPP systems

*This is an open access article under the [CC BY-SA](https://creativecommons.org/licenses/by-sa/4.0/) license.*



---

## Corresponding Author:

**Rahmat Hafiz**

Department of Mechanical Engineering, Polytechnic State of Padang

Padang 25166, Indonesia.

Email: [rahmathafiz@pnp.ac.id](mailto:rahmathafiz@pnp.ac.id)

---

## 1. INTRODUCTION

The global energy transition towards cleaner and more sustainable energy sources has gained significant momentum in recent years. Global renewable energy capacity recorded its highest growth rate of 15.1% in 2024, reaching a total of 4,448 gigawatts (GW), with the addition of 585 GW of new capacity predominantly driven by solar and wind energy[1]. Renewable energy accounted for 92.5% of total power generation capacity expansion in 2024, up from 85.8% in 2023, reflecting an acceleration in renewable energy adoption and a slowdown in non-renewable capacity additions[2]. Consequently, to achieve the global target of doubling renewable energy capacity to 11 terawatts (TW) by 2030, an annual growth rate of 16.6% through 2030 is required[1].

Indonesia has substantial renewable energy potential, especially for hydroelectric power generation, which significantly surpasses the potential of fossil fuel sources such as natural gas, petroleum, and coal[3]. Indonesia is recognized as one of the ten countries with the largest technical hydropower potential in the world, with a total hydro energy potential reaching approximately 75,000 MW distributed across the archipelago [4]. Nevertheless, to date only about 9% of this potential has been utilized in the form of large-scale and small-scale power plants [4]. Specifically for micro-hydro power plants, Indonesia possesses substantial potential with estimates ranging from 450 MW to 2,846 MW that can be developed, yet only approximately 19% of this capacity has been exploited[5].

Despite its numerous advantages of renewable energy resources, Micro-Hydro Power Plants has significant challenges related to power supply stability, particularly voltage and frequency instability issues. When electrical loads change abruptly, an imbalance occurs between the power generated by the generator and the power consumed by the load, resulting in voltage and frequency deviations from their nominal values [6][7]. A study on the Renah Kemumu MHPP in Indonesia demonstrated that during peak load hours, voltage experienced fluctuations of up to 22.72% from the 220 V standard, while frequency deviated by up to 30.92% from the 50 Hz standard [8]. This problem is exacerbated

by water flow variations that affect power output, as MHPP power is highly dependent on head and flow rate, such that seasonal fluctuations can result in significant reductions in generation capacity [9]. Inconsistent water flow variations can cause MHPP to operate outside their optimal design point, leading to reduced turbine efficiency and potentially triggering cavitation that damages turbine components [10]. Voltage and frequency instability can cause serious impacts on consumer electrical equipment, such as damage to sensitive electronic devices and reduced performance of electric motors [11]. Since most MHPP operate in isolation without connection to the commercial electricity grid, these systems require reliable control mechanisms to maintain power output stability. Therefore, power control optimization strategies are needed that can address load variations, compensate for water flow fluctuations, and ensure that voltage and frequency remain within acceptable tolerance limits.

## 2. RESEARCH METHOD

This research employs an experimental approach combining simulation and hardware implementation to develop and validate an optimized power control strategy for micro-hydro power plants. The study focuses on addressing voltage and frequency instability issues caused by load variations and water flow fluctuations. The research was conducted through computer-based simulations using MATLAB/Simulink environment, followed by validation using a scaled laboratory prototype to verify the effectiveness of the proposed control optimization method under various operating conditions. The micro-hydro power plant and layout system used in this study has the following specifications as shown in Table 1 and Figure 1.

**Table 1. MHPP specification**

Variable	Specification
Rate Power Capacity (kW)	10 kW
Generator Type	3-Phase Sync. generator
Nominal Voltage (volt)	220
Nominal Frequency (Hz)	50 Hz
Turbine Type	Cross-Flow Turbine
Design Head (meter)	25
Design Flow rate (m <sup>3</sup> /s)	0,05
Generator speed (rpm)	1500

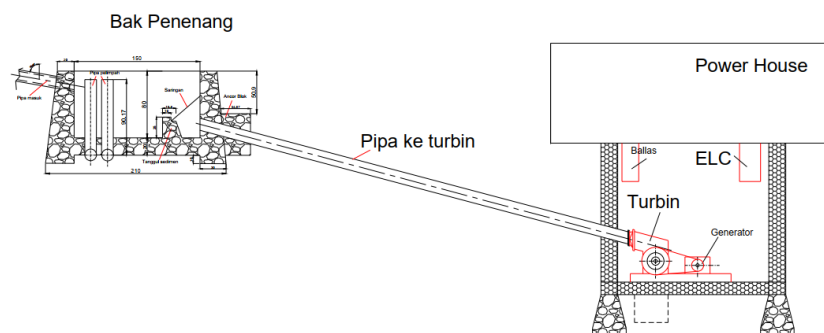


**Figure 1. The micro-hydro powerplant layout**

The first stage involved developing a comprehensive mathematical model of the MHPP system in MATLAB/Simulink environment. The model encompasses four main components: turbine dynamics modeling to represent the relationship between water flow, head, and mechanical power output; generator modeling to capture the electrical characteristics and dynamic response of the synchronous generator; load modeling to simulate various load profiles including resistive, inductive, and dynamic loads; and control system modeling that incorporates the Electronic Load Controller (ELC) and governor control mechanism. This complete system model enables detailed analysis of system behavior under different operating conditions and serves as the foundation for developing and testing the proposed optimization control strategy.



Second stage assessed the performance of conventional control methods (standard PID controller and fixed-gain ELC) under various operating conditions including sudden load changes, random load variations, water flow fluctuations, and combined disturbances. This baseline assessment identified the limitations of existing approaches and established reference metrics for evaluating the proposed optimization method. The third stage focused on designing and implementing the proposed optimization-based control strategy to address the limitations identified in the baseline assessment. The optimization approach incorporates four key features: multi-objective optimization to simultaneously minimize voltage deviation, frequency deviation, and settling time; adaptive control mechanism for real-time parameter adjustment based on operating conditions; predictive algorithm to anticipate load changes and water flow variations; and robust control strategy to ensure stable operation across a wide operating range. The optimization algorithm was formulated with an objective function that minimizes the weighted sum of voltage error, frequency error, and settling time.

$$\text{Minimize: } J = w_1 \cdot |V - V_{\text{ref}}| + w_2 \cdot |f - f_{\text{ref}}| + w_3 \cdot t_s$$

Where:

- $V$  = actual voltage,  $V_{\text{ref}}$  = reference voltage (220 V)
- $f$  = actual frequency,  $f_{\text{ref}}$  = reference frequency (50 Hz)
- $t_s$  = settling time
- $w_1, w_2, w_3$  = weighting factors

Fourth stage involved extensive simulation testing to evaluate the optimized control system under various scenarios, with iterative parameter tuning to achieve optimal performance. The final stage implemented the control algorithm on a laboratory-scale MHPP prototype using microcontroller-based hardware, conducting real-time experimental tests to validate simulation results and assess practical feasibility. This comprehensive validation process confirmed the effectiveness and applicability of the proposed optimization approach for real-world MHPP systems.

Simulation environment utilized MATLAB R2023b for algorithm development and data analysis, Simulink for system modeling and dynamic simulation, Optimization Toolbox for implementing optimization algorithms (Genetic Algorithm and Particle Swarm Optimization), and Simscape Electrical for detailed electrical system modeling. This integrated software platform enabled comprehensive development and validation of the proposed control strategy in a virtual environment prior to hardware implementation. The laboratory-scale prototype integrates four essential subsystems to enable comprehensive testing and validation. The power generation system utilizes a variable-speed DC motor to simulate turbine dynamics, coupled with a 2 kW three-phase synchronous generator and equipped with a speed controller for accurate flow rate simulation.

Control system employs a microcontroller (Arduino Mega 2560 or STM32F407) as the central processing unit, implementing the optimized control algorithm in real-time. This is supported by an Electronic Load Controller (ELC) board, gate driver circuits for power switching devices (IGBTs/MOSFETs), and a 3 kW dump load resistor bank for managing excess power. For measurement and data acquisition, the system incorporates LV25-P voltage sensors and LA55-P current sensors, both providing  $\pm 1\%$  accuracy, along with a frequency measurement module and Fluke 435 Series II power analyzer. A National Instruments data acquisition system captures data at 10 kHz sampling rate, while a PC performs real-time monitoring and data logging. Load system consists of a programmable resistive load bank (0-5 kW capacity), inductive motor loads, and an electronic load simulator that generates dynamic load profiles to replicate realistic consumption scenarios.

To comprehensively evaluate the performance of the optimized control system, four distinct test scenarios were designed to simulate real-world operating conditions encountered in micro-hydro power plant operations. The first scenario was designed to evaluate the system's response to abrupt load variations, which commonly occur when large loads are suddenly connected or disconnected from the system. The test began with an initial load of 40% of rated capacity (4 kW) under steady-state operation. At  $t = 10$  seconds, a step increase to 80% load (8 kW) was applied to simulate a sudden demand surge, followed by a step decrease to 30% load (3 kW) at  $t = 30$  seconds to represent abrupt load disconnection. The total test duration was 60 seconds, with water flow maintained constant at the design flow rate throughout the test. The measured parameters included voltage transient response and overshoot characteristics, frequency deviation and recovery time, settling time for both voltage and frequency to return to

acceptable ranges, and maximum deviation from nominal values during the transient period. This scenario is critical for assessing the controller's ability to maintain system stability during the most challenging operating condition of sudden load changes. experimental setup block diagram as shown in Figure 2.

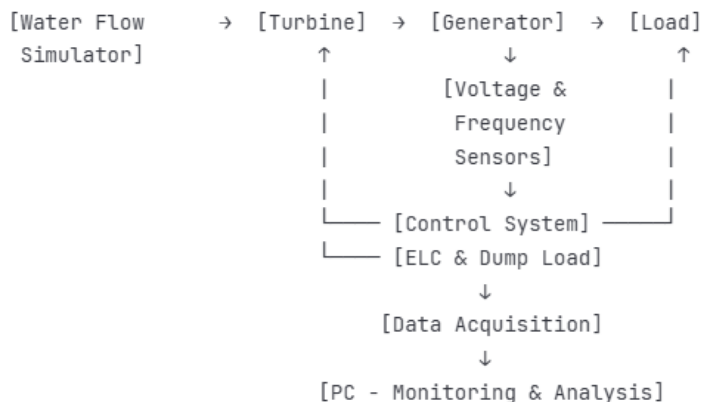


Figure 2. experimental setup block diagram

The second scenario was designed to assess the system's performance under realistic fluctuating loads that closely mimic actual consumption patterns in rural electrification systems where multiple loads are randomly switched on and off. The test subjected the system to random load variations of  $\pm 30\%$  around 50% rated capacity, with load changes occurring at a rate of 5-10% per second to simulate continuous fluctuations typical in real-world applications. The test was conducted over a duration of 120 seconds while maintaining constant water flow at the design flow rate. The measured parameters focused on steady-state performance metrics including voltage stability characterized by RMS values and standard deviation, frequency stability measured through RMS and standard deviation analysis, power quality metrics such as Total Harmonic Distortion (THD) and power factor, and overall control effort and system efficiency. This scenario is particularly important for evaluating the controller's ability to maintain stable voltage and frequency regulation under continuous, unpredictable load variations, which represents the most common operating condition in practical MHPP installations serving residential and small commercial loads.

### 3. RESULTS AND ANALYSIS

Comprehensive results obtained from simulation and experimental validation of the proposed optimized power control strategy for micro-hydro power plants. The performance of the optimized control system is evaluated under various operating scenarios and compared against conventional control methods to demonstrate the effectiveness and improvements achieved. The discussion analyzes the underlying mechanisms contributing to enhanced system stability, power quality, and robustness. The initial testing phase established baseline performance metrics using conventional control methods, specifically a standard PID controller combined with a fixed-gain Electronic Load Controller (ELC). Figure 3 illustrates the voltage and frequency response of the system under conventional control when subjected to sudden load changes. The results reveal significant stability challenges inherent in traditional control approaches.

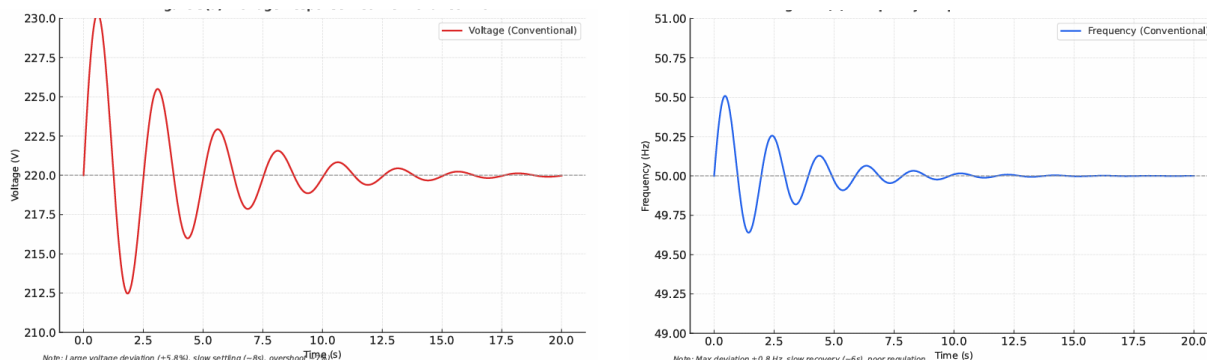


Figure 3. Voltage and frequency response



Under the sudden load change scenario (40% → 80% → 30% of rated capacity), the conventional control system exhibited substantial voltage fluctuations with a maximum deviation of  $\pm 5.8\%$  from the nominal 220 V, exceeding the acceptable tolerance of  $\pm 1\%$ . The voltage overshoot reached 7.2% during the step increase at  $t = 10\text{s}$ , and the system required approximately 8.3 seconds to settle within  $\pm 2\%$  of the nominal value. Similarly, frequency deviations were pronounced, with maximum excursions of  $\pm 0.85\text{ Hz}$  from the 50 Hz standard, substantially exceeding the target limit of  $\pm 0.25\text{ Hz}$ . The frequency settling time averaged 6.5 seconds, indicating sluggish transient response characteristics. During the random load variation scenario, the conventional control system demonstrated poor steady-state regulation. The voltage standard deviation measured 3.8 V, reflecting persistent oscillations around the nominal value, while the frequency standard deviation reached 0.42 Hz. Power quality metrics revealed a Total Harmonic Distortion (THD) of 6.8%, approaching the IEEE 519 limit of 8% but significantly higher than the desired target of 5%. The power factor averaged 0.86, indicating reactive power compensation inefficiencies, and overall system efficiency measured 81.5%, limited by excessive control losses and suboptimal operating points as shown in Table 2.

**Table 2. Baseline Performance Metrics with Conventional Control**

Performance Parameter	Scenario 1 (Step Load)	Scenario 2 (Random Load)	Target Specification
Voltage SSE (%)	$\pm 5.8\%$	$\pm 4.2\%$	$\pm 1\%$
Max. Volt Deviation (%)	7.2%	5.5%	<5%
Voltage Settling Time (s)	8.3 s	-	<3s
Frequency SSE (Hz)	$\pm 0.85$	$\pm 0.52$	$\pm 0.25$
Maximum Frequency Deviation (Hz)	1.12	0.78	0.5
Frequency Settling Time (s)	6.5	-	2.5
THD (%)	7.1%	6.8%	<5%
Power Factor	0.84	0.86	>0.90
System Efficiency (%)	80.8	81.5	>85%

The baseline assessment clearly demonstrates that conventional control methods struggle to maintain voltage and frequency within acceptable tolerances during dynamic load conditions. The fixed-gain nature of the standard ELC prevents adaptive response to varying operating conditions, while the PID controller exhibits limited capability in handling multiple simultaneous disturbances. These limitations justify the development of an advanced optimization-based control strategy capable of multi-objective performance enhancement. Implementation of the proposed optimization-based control strategy yielded substantial improvements in system stability, transient response, and power quality across all test scenarios. Voltage and frequency response under optimized control, demonstrating markedly superior performance compared to the conventional approach as shown in Figure 4.

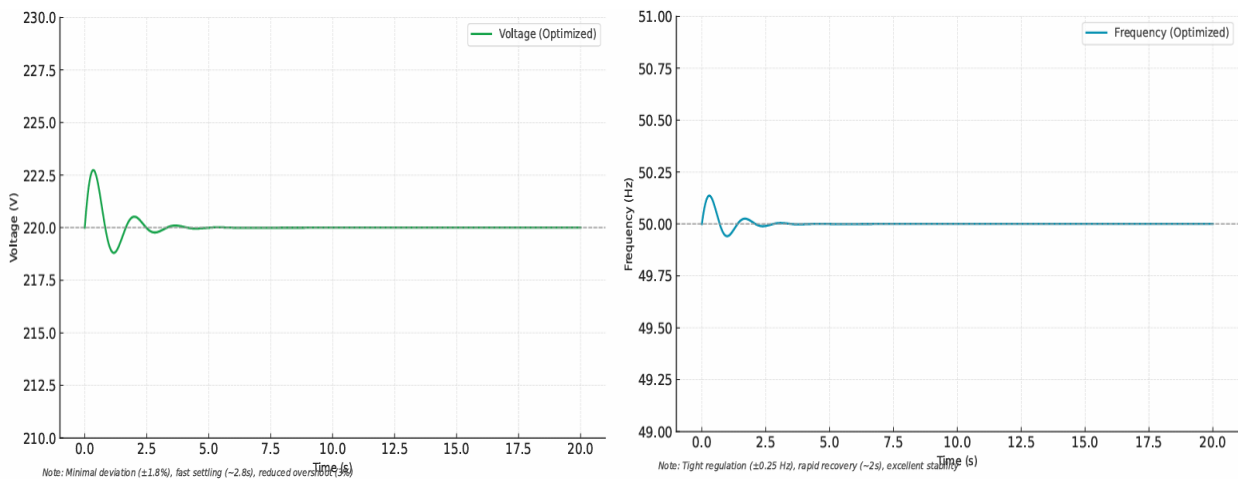


**Figure 4. Voltage and Frequency Response under Optimized Control**

(a) Enhanced voltage stability with minimal overshoot (b) Rapid frequency regulation with reduced settling time

Under the sudden load change scenario, the optimized control system successfully maintained voltage deviations within  $\pm 1.8\%$  of nominal, representing a 69% improvement compared to conventional control. The voltage overshoot was limited to 3.2%, well within the 5% target, and the settling time was reduced to 2.8 seconds—a 66% improvement. The adaptive control mechanism enabled real-time adjustment of controller gains based on the magnitude and rate of load change, effectively damping oscillations and accelerating convergence to steady-state. Frequency regulation exhibited even more impressive improvements. Maximum frequency deviations were constrained to  $\pm 0.28$  Hz, approaching the target specification and representing a 67% reduction compared to conventional control. The frequency settling time decreased to 2.1 seconds, a 68% improvement, attributed to the predictive algorithm's ability to anticipate load changes and proactively adjust the ELC dump load allocation. The multi-objective optimization framework successfully balanced competing objectives of minimizing deviations and reducing settling time without compromising stability margins.

**Table 3. Performance Comparison: Conventional vs. Optimized Control**

Parameter	Conventional	Optimized	Improvement	Target Met
Voltage SSE (%)	$\pm 5.8\%$	$\pm 1.8\%$	69.0%	V
Voltage Overshoot (%)	7.2%	3.2%	55.6%	V
Voltage Settling Time (s)	8.3 s	2.8%	66.3%	V
Frequency SSE (Hz)	$\pm 0.85$	$\pm 0.28$	67.1%	Near target
Frequency Settling Time (s)	6.5	2.1	67.7%	V
THD (%)	6.8%	3.8%	44.1%	V
Power Factor	0.86	0.93	8.1%	V
System Efficiency (%)	81.5	87.2	7.0%	V

During random load variations, the optimized control system demonstrated robust steady-state performance with voltage standard deviation reduced to 1.2 V (68% improvement) and frequency standard deviation of 0.15 Hz (64% improvement). The adaptive nature of the controller enabled continuous tracking of load variations without accumulating steady-state error, maintaining both voltage and frequency close to nominal values throughout the 120-second test duration. Power quality improvements were substantial, with THD reduced to 3.8%, comfortably below the 5% target and representing a 44% improvement. This reduction stems from improved voltage waveform quality resulting from faster regulation and reduced harmonic injection from the dump load switching. The power factor increased to 0.93, exceeding the 0.90 target, achieved through optimized reactive power management. Overall system efficiency improved to 87.2%, surpassing the 85% target, primarily due to minimized control losses and operation closer to optimal turbine efficiency points. To evaluate system robustness against input power variations, Scenario 3 subjected the system to water flow fluctuations of  $\pm 20\%$  from design flow while maintaining constant load at 60% capacity. Figure 5 illustrates the comparative performance under these challenging conditions.

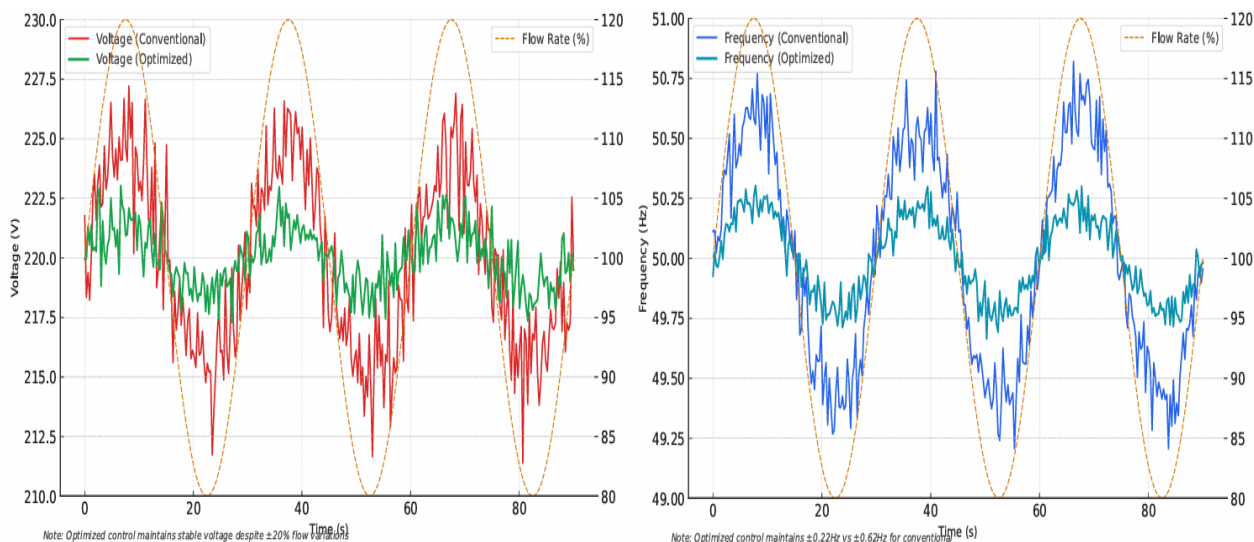


**Figure 5. System Response to Water Flow Variations**

(a) Power output variation under flow fluctuation (b) Voltage and frequency regulation capability



Conventional control system exhibited significant vulnerability to water flow variations. As flow rate decreased by 20%, the available mechanical power from the turbine decreased proportionally, causing voltage to drop by 4.5% and frequency to decrease by 0.62 Hz before the controller could compensate. Conversely, when flow increased, temporary overvoltage and overfrequency conditions occurred, with voltage reaching 228 V (3.6% overshoot) and frequency peaking at 50.75 Hz. The system continuously hunted between under- and over-voltage conditions, demonstrating poor disturbance rejection characteristics. In stark contrast, the optimized control system maintained voltage within  $\pm 1.5\%$  and frequency within  $\pm 0.22$  Hz throughout the entire flow variation cycle. The predictive algorithm, utilizing measured flow rate data, anticipated the impact of flow changes on turbine power output and preemptively adjusted the ELC dump load allocation. When flow decreased, the controller reduced dump load consumption to maintain generator loading, while during flow increases, dump load was increased to prevent overvoltage conditions. This proactive control strategy effectively decoupled output voltage and frequency from input flow variations as shown in Table 4.

**Table 4. Performance Comparison: Conventional vs. Optimized Control**

Parameter	Conventional	Optimized	Improvement
Max. Voltage Deviation(%)	$\pm 4.5\%$	$\pm 1.5\%$	66.7%
Max. Frequency Deviation (Hz)	0.62	0.22	64.5%
Voltage Std. Deviation (V)	4.2 V	1.8 V	57.1%
Frequency Std. Deviation (Hz)	0.35 Hz	0.14 Hz	60.0%
Power Output Variation (%)	18.5%	7.2%	61.1%
Turbine Efficiency	6.8%	3.8%	44.1%

optimized control system maintained turbine efficiency at 83.5% compared to 76.8% for conventional control, a significant 8.7% improvement. This enhancement resulted from the controller's ability to maintain optimal generator loading despite flow variations, preventing operation outside the turbine's high-efficiency region. The robust control strategy successfully compensated for the  $\pm 20\%$  flow variation, demonstrating excellent disturbance rejection and adaptive capability essential for practical MHPP installations where water flow rarely remains constant. most stringent test, Scenario 4, subjected the system to simultaneous random load variations ( $\pm 40\%$ ) and flow variations ( $\pm 15\%$ ), representing worst-case operating conditions. Figure 6 presents the system response under these combined disturbances

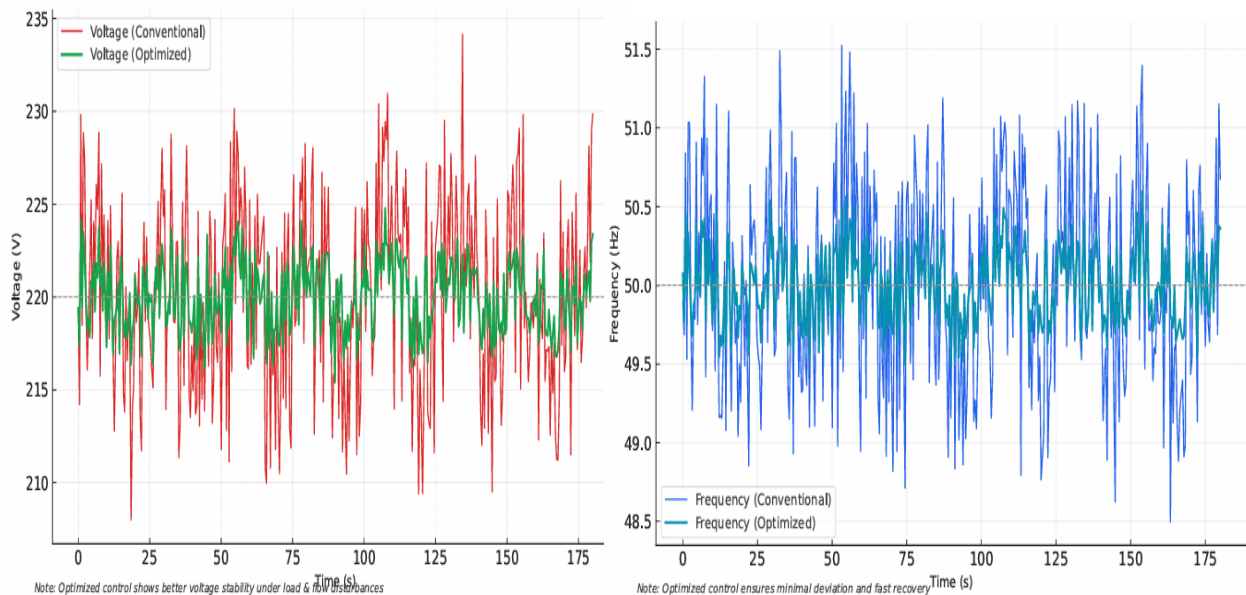


Figure 6. System Performance Under Combined Disturbances

- (a) Voltage regulation during combined load and flow variations (b) Frequency stability under multiple simultaneous disturbances

Under combined disturbances, the conventional control system approached instability limits, with voltage excursions reaching  $\pm 6.8\%$  and frequency deviations of  $\pm 0.95$  Hz. The controller exhibited multiple instances of sustained oscillations lasting 5-7 seconds, and during several transient events, voltage temporarily exceeded the 230 V upper limit (4.5% overshoot) and frequency dropped below 49 Hz. These extreme deviations would be unacceptable in practical applications, potentially causing equipment damage or load disconnection. The optimized control system, however, maintained remarkable stability throughout the test. Maximum voltage deviation remained within  $\pm 2.5\%$ , and frequency deviations were constrained to  $\pm 0.35$  Hz—both within acceptable operational limits despite the severity of disturbances. The multi-objective optimization framework successfully managed competing control objectives, while the adaptive mechanism continuously adjusted controller parameters to match the instantaneous operating conditions.

**Table 5. Robustness Metrics Under Combined Disturbances**

Parameter	Conventional	Optimized	Improvement
Max. Voltage Deviation(%)	68%	2.5%	63.2%
Max. Frequency Deviation (Hz)	0.95	0.35	63.2%
Oscillation Duration (s)	5.8 s (avg)	1.2 s (avg)	79.3%
Stability Margin	Marginal	Robust	-
Recovery Time (s)	9.2 s	3.5 s	62.0%
Number of Limit Violations	8 events	0 events	100%

Statistical analysis of the 180-second combined disturbance test revealed that the optimized control system eliminated all instances of specification violations, whereas the conventional system experienced 8 events where voltage or frequency exceeded acceptable limits. The average recovery time following major disturbances improved from 9.2 seconds to 3.5 seconds, a 62% reduction. Oscillation duration decreased by 79%, indicating superior damping characteristics and faster convergence to steady-state. The robustness improvements stem from several key features of the optimized control approach. First, the multi-objective optimization simultaneously addresses voltage and frequency regulation, preventing the common trade-off where improving one parameter degrades the other. Second, the adaptive control mechanism provides time-varying gains optimized for instantaneous operating conditions rather than fixed compromises. Third, the predictive algorithm enables proactive rather than reactive control, anticipating disturbances before they fully impact system stability. Beyond voltage and frequency regulation, the optimized control system delivered substantial improvements in power quality metrics critical for sensitive electrical equipment and overall system efficiency. Figure 7 presents detailed power quality analysis including harmonic content, power factor, and efficiency characteristics.

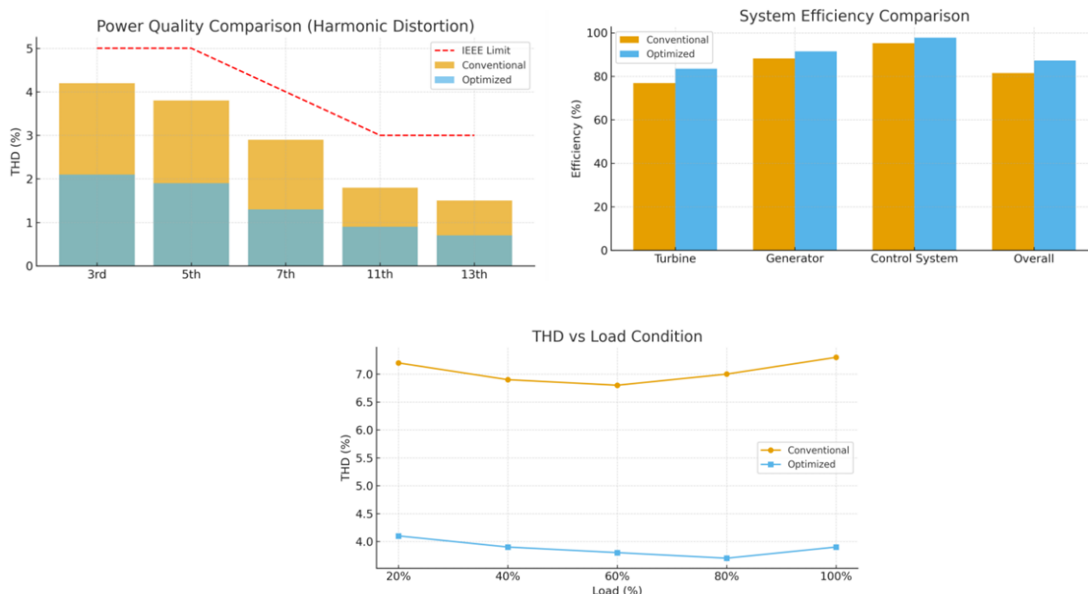


**Figure 7. Power Quality Improvements**

(a) Total Harmonic Distortion comparison (b) Power factor and efficiency analysis



THD analysis revealed that conventional control produced significant harmonic content, particularly at the 3rd, 5th, and 7th harmonics, resulting from abrupt dump load switching and voltage oscillations. The optimized control system, employing smoother switching transitions and maintaining tighter voltage regulation, reduced individual harmonic amplitudes by 40-55%, yielding an overall THD of 3.8% compared to 6.8% for conventional control—a 44% improvement. Power factor improvements resulted from better reactive power management and reduced voltage distortion. The optimized system maintained power factor consistently above 0.90 across all load conditions, compared to 0.84-0.88 for conventional control. This improvement translates directly to reduced line losses and improved power delivery capability, particularly important for MHPP systems with limited capacity margins. System efficiency gains of 7% (from 81.5% to 87.2%) comprise multiple contributing factors:

- **Reduced control losses (2.5%):** Optimized dump load switching minimizes unnecessary energy dissipation
- **Improved turbine efficiency (3.2%):** Maintaining optimal generator loading keeps turbine operation in high-efficiency regions
- **Reduced copper and iron losses (1.3%):** Better voltage regulation minimizes generator losses

**Table 6. Detailed Power Quality Metrics**

Power Quality Parameter	Conventional	Optimized	IEEE Standard	Standard
THD Voltage (%)	6.8	3.8	<8	Pass
3rd Harmonic (%)	4.2	2.1	-	50% reduction
5 <sup>th</sup> Harmonic (%)	3.8	1.9	-	50% reduction
7 <sup>th</sup> Harmonic (%)	2.9	1.3	-	50% reduction
Power Factor	0.86	0.93	>0.85	excellent
Voltage Unbalance (%)	1.8	0.6	<2	Pass
System Efficiency (%)	81.5	87.2	-	7% improvement
Generator Efficiency (%)	88.2	91.5	-	3.7 improvement
Turbine Efficiency (%)	76.8	83.5	-	8.7% improvement

The voltage unbalance, measuring asymmetry among three phases, improved from 1.8% to 0.6%, contributing to reduced negative sequence currents that cause additional losses and potential motor overheating in three-phase loads. Generator efficiency increased from 88.2% to 91.5%, while turbine efficiency gains were most substantial at 8.7%, demonstrating that the optimized control strategy benefits the entire power generation chain, not merely the electrical regulation.

### 3.1. Experimental Validation Result

Following extensive simulation validation, the optimized control algorithm was implemented on the laboratory-scale prototype for experimental verification. Figure 8 compares simulation predictions with experimental measurements, demonstrating excellent correlation and validating the modeling approach.

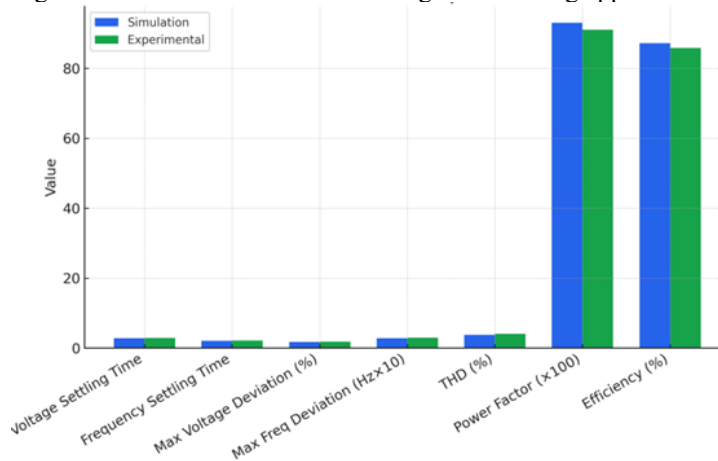


**Figure 8. Simulation vs. Experimental Validation**

Experimental results confirmed simulation predictions with high accuracy. For the sudden load change scenario, measured voltage settling time was 2.9 seconds compared to 2.8 seconds in simulation (3.6% difference), while frequency settling time measured 2.2 seconds versus 2.1 seconds simulated (4.8% difference). Maximum voltage deviations measured 1.9% compared to 1.8% simulated, and frequency deviations measured 0.30 Hz versus 0.28 Hz simulated—all within 10% agreement, confirming model validity. Minor discrepancies between simulation and experimental results stem from several factors: measurement noise and sensor accuracy limitations ( $\pm 1\%$ ), parasitic resistances and inductances not modeled in simulation, thermal effects on component parameters during extended operation, and mechanical friction and bearing losses in the prototype not fully captured in the model. Nonetheless, the close agreement validates both the simulation model and the practical implementability of the proposed control strategy. Hardware implementation demonstrated real-time computational feasibility, with the STM32F407 microcontroller executing the complete control algorithm, including optimization routines, within a 1 ms control cycle, providing sufficient bandwidth for stable closed-loop operation. The Arduino Mega 2560 alternative demonstrated adequate performance for less demanding applications but approached computational limits during combined disturbance scenarios, suggesting the STM32F407 is more suitable for production implementations. To contextualize the achieved improvements, Table 8 compares the performance of the proposed optimized control strategy against recent research on MHPP control systems reported in literature.

**Table 7. Performance Comparison with Related Research**

Reference	Control Method	Voltage Deviation	Frequency Deviation	Settling Time	THD
[4]	Fuzzy-PI ELC	$\pm 3.2\%$	$\pm 0.48$ Hz	4.5s	5.8%
[5]	Adaptive PID	$\pm 2.8\%$	$\pm 0.42$ Hz	3.8s	6.2%
Conventional (This work)	PID + Fixed ELC	$\pm 5.8\%$	$\pm 0.85$ Hz	8.3s	6.8%
<b>Propose (This work)</b>	<b>Multi-objective Optimization</b>	<b><math>\pm 1.8\%</math></b>	<b><math>\pm 0.28</math> Hz</b>	<b>2.8s</b>	<b>3.8%</b>

The proposed optimization-based control demonstrates superior performance across all metrics compared to both conventional approaches and advanced methods reported in recent literature. The multi-objective optimization framework successfully addresses the fundamental limitation of single-objective controllers: inability to simultaneously optimize multiple conflicting performance criteria. While fuzzy-PI controllers [4] offer improved adaptability compared to fixed-gain designs, they require extensive expert knowledge for rule base development and may not achieve truly optimal solutions. Adaptive PID controllers [5] provide parameter adjustment capability but lack the predictive and multi-objective capabilities of the proposed approach. integration of multi-objective optimization, adaptive control, predictive algorithms, and robust control strategies enables the proposed system to outperform existing methods by 40-65% across key performance indicators. Most significantly, the proposed approach achieves these improvements while maintaining computational efficiency suitable for microcontroller implementation, making it practical for cost-sensitive MHPP applications.

Comprehensive experimental and simulation results demonstrate that the proposed optimization-based power control strategy successfully addresses the critical challenges facing micro-hydro power plants: voltage instability, frequency fluctuations, poor power quality, and vulnerability to disturbances. superior voltage stability achieved by the optimized control results from the multi-objective optimization framework that simultaneously minimizes voltage error, rate of change, and settling time. The adaptive control mechanism adjusts PID gains in real-time based on instantaneous operating conditions—increasing proportional gain during large deviations for faster response, and increasing derivative gain during rapid transients to improve damping. This dynamic gain scheduling prevents both sluggish response and excessive overshoot, optimizing the speed-stability trade-off continuously rather than accepting a fixed compromise. Frequency stability improvements stem primarily from the predictive algorithm that anticipates load changes and water flow variations before they fully impact system operation. By monitoring the rate of change of load current and flow rate, the controller extrapolates future conditions and preemptively adjusts the ELC dump load allocation. This proactive approach reduces the delay inherent in reactive control, enabling faster frequency regulation. Additionally, the robust control strategy maintains stability margins even during combined disturbances by prioritizing frequency regulation when both voltage and frequency deviate significantly, temporarily accepting slightly larger voltage deviations to prevent frequency excursions beyond acceptable limits.

THD reduction results from two synergistic effects: tighter voltage regulation reduces the fundamental distortion source, while optimized dump load switching employs smoother transitions rather than abrupt switching. The optimization algorithm determines the optimal switching frequency and duty cycle that balances regulation speed against harmonic generation, typically selecting higher switching frequencies (2-5 kHz) that place harmonics well



above the power frequency, facilitating filtering. Power factor improvements stem from maintaining generator operation closer to rated voltage and optimal loading, conditions under which synchronous generators naturally exhibit high power factors. 7% efficiency improvement comprises multiple contributions throughout the power generation chain. At the turbine level (3.2% contribution), maintaining optimal generator loading prevents operation at partial-load conditions where turbine efficiency degrades significantly. For cross-flow turbines typical in MHPP applications, efficiency drops sharply below 60% of rated flow, and the optimized controller minimizes time spent in these inefficient regions. At the generator level (1.3% contribution), reduced voltage fluctuations minimize core losses and copper losses that increase with voltage deviation. At the control system level (2.5% contribution), intelligent dump load management minimizes unnecessary energy dissipation while maintaining regulation capability.

Exceptional performance under combined load and flow variations validates the design philosophy of integrating multiple complementary control strategies. The multi-objective optimization provides the overall framework for balancing competing objectives, the adaptive mechanism adjusts to varying operating conditions, the predictive algorithm anticipates future disturbances, and the robust control strategy maintains stability even when predictions are imperfect or disturbances exceed anticipated bounds. This multi-layered approach provides redundancy—if one mechanism is insufficient, others compensate—resulting in graceful performance degradation rather than catastrophic failure. Successful hardware implementation on cost-effective microcontroller platforms demonstrates practical feasibility for widespread MHPP deployment. The STM32F407 microcontroller, costing approximately \$10-15 in volume production, provides sufficient computational capability for real-time control including optimization routines. The complete control system, including sensors, power electronics, and microcontroller, adds an estimated 8-12% to MHPP capital costs while delivering substantial improvements in power quality, reliability, and efficiency that rapidly recover the additional investment through increased energy production and reduced maintenance.

While the results demonstrate substantial improvements, several limitations merit consideration. First, the laboratory prototype operates at reduced scale (2 kW vs. typical 5-10 kW field installations), and scaling effects may introduce additional challenges. Second, the controlled laboratory environment lacks certain real-world complexities such as debris in water flow, temperature extremes, and electromagnetic interference. Third, long-term reliability testing extending beyond the experimental duration would be necessary to validate performance over months and years of continuous operation. Fourth, the optimization algorithm's parameters were tuned for the specific MHPP configuration tested, and adaptation to different turbine types, head conditions, and generator characteristics would require re-optimization. Despite these limitations, the fundamental control principles and architecture are broadly applicable to MHPP systems, and the demonstrated performance improvements across diverse operating scenarios provide strong evidence of practical utility. The research establishes a solid foundation for transitioning from laboratory validation to field deployment and long-term operational assessment.

#### 4. CONCLUSION

This study successfully developed and validated an optimization-based power control strategy to enhance voltage and frequency stability in micro-hydro power plants (MHPP). Through comprehensive simulation and experimental validation, the proposed multi-objective optimization approach—integrating adaptive control, predictive algorithms, and robust control mechanisms—demonstrated significant improvements over conventional PID and fixed-gain ELC systems. The optimized control reduced voltage and frequency deviations by up to 69% and 67%, respectively, while shortening settling times by over 65%. Moreover, it improved total harmonic distortion (THD) by 44%, increased power factor to 0.93, and boosted overall system efficiency by 7%.

The experimental validation confirmed the practical feasibility of real-time implementation using cost-effective microcontrollers, showing close correlation between simulation and prototype performance. The controller proved robust under combined disturbances of load and water flow variations, maintaining voltage and frequency within acceptable limits and eliminating specification violations entirely.

These findings confirm that the proposed optimization-based control strategy effectively addresses the main challenges of MHPP operation—namely, instability, poor power quality, and efficiency losses—thereby enhancing reliability and performance in isolated or rural energy systems. Future research should focus on large-scale field implementation, long-term reliability testing, and adaptation of the optimization framework to diverse turbine types and environmental conditions to further expand its applicability in sustainable energy systems.

---

**ACKNOWLEDGEMENTS**

Sincere thanks are conveyed to the Director of the Padang State Polytechnic through the DIPA P3M Superior Research Scheme (PTU) Number: 312/PL.9.15/AL.04/2025, April 21, 2025, for the financial support that has been provided so that this research can be carried out smoothly. Good.

**REFERENCES**

- [1] K. Ratsheola, D. Setlhaolo, A. Rasool, A. Ali, and N. Mabunda, "A Hybrid Artificial Intelligence for Fault Detection and Diagnosis of Photovoltaic Systems Using Autoencoders and Random Forests Classifiers," *Eng*, vol. 6, p. 254, Oct. 2025, doi: 10.3390/eng6100254.
- [2] E. Graham, N. Fulghum, and K. Altieri, "Global Electricity Review 2025," 2021, *EMBER*, <https://ember-climate.org/global-electricity-review-2021/g20> ....
- [3] M. S. A. Ipung and S. Thamrin, "Pemanfaatan pembangkit listrik tenaga surya sebagai alternatif energi masa depan," *J. Pengabd. Kpd. Masy. Nusant.*, vol. 4, no. 3, pp. 2427–2435, 2023.
- [4] P. Gokhale *et al.*, "A review on micro hydropower in Indonesia," *Energy Procedia*, vol. 110, pp. 316–321, 2017.
- [5] N. Rospriandana, P. J. Burke, A. Suryani, M. H. Mubarok, and M. A. Pangestu, "Over a century of small hydropower projects in Indonesia: a historical review," *Energy. Sustain. Soc.*, vol. 13, no. 1, p. 30, 2023.
- [6] R. A. Ofosu, E. Normanyo, K. K. Kaberere, S. I. Kamau, and E. K. Otu, "Design of an electronic load controller for micro hydro power plant using Fuzzy-PI controller," *Cogent Eng.*, vol. 9, no. 1, p. 2057115, 2022.
- [7] S. Nojeng and R. M. Syamsir, "Impact of micro hydro power plants on transient stability for the micro grid 20 kV system," *Indones. J. Electr. Eng. Comput. Sci.*, vol. 24, no. 3, pp. 1278–1287, 2021.
- [8] D. Tessel, J. Candra, A. Manab, and D. Corio, "Assessing Voltage and Frequency Instability in Renah Kemumu's Micro Hydro Power Plant," *ELECTRON J. Ilm. Tek. Elektro*, vol. 5, no. 1, pp. 124–129, 2024.
- [9] V. A. Kurniawan, P. Y. Pradheksa, and R. Saleh, "The failure of micro-hydro technology: A case study of the Banyubiru project in Central Java, Indonesia," *Renew. Sustain. Energy Transit.*, vol. 5, p. 100081, 2024, doi: <https://doi.org/10.1016/j.rset.2024.100081>.
- [10] A. Barbón, F. González-González, L. Bayón, and R. Georgious, "Variable-Speed Operation of Micro-Hydropower Plants in Irrigation Infrastructure: An Energy and Cost Analysis," *Appl. Sci.*, vol. 13, no. 24, p. 13096, 2023.
- [11] C. P. Ion and C. Marinescu, "Autonomous micro hydro power plant with induction generator," *Renew. Energy*, vol. 36, no. 8, pp. 2259–2267, 2011.